

## Article

# Assessment of the Possibilities for Removal of Ni (II) from Contaminated Water by Activated Carbon foam Derived from Treatment Products of RDF

Ivanka Stoycheva \*, Boyko Tsyntsarski, Angelina Kosateva, Bilyana Petrova and Pavlinka Dolashka

Institute of Organic Chemistry with Centre of Phytochemistry, Bulgarian Academy of Sciences, Acad. G. Bonchev Str. BL.9, 1113 Sofia, Bulgaria; boyko.tsyntsarski@orgchm.bas.bg (B.T.); angelina.kosateva@orgchm.bas.bg (A.K.); bilyana.petrova@orgchm.bas.bg (B.P.); pavlina.dolashka@orgchm.bas.bg (P.D.)

\* Correspondence: ivanka.stoycheva@orgchm.bas.bg

**Abstract:** Carbon foam is a sophisticated porous material with wide applications that depend on its structure, low density, thermal conductivity and electrical characteristics. This study deals with the preparation of carbon foam by the thermo-oxidative modification with HNO<sub>3</sub> of mixtures containing different organic materials with appropriate chemical characteristics—furfural and tar pitch derived from RDF. Carbon foam is characterized by thermogravimetry, differential scanning calorimetry, elemental analysis, Raman spectroscopy, N<sub>2</sub> sorption, infrared spectroscopy and scanning electron spectroscopy. The investigation of adsorption activity of carbon foam towards nickel (II) in water solution is carried out. Experimental results fit very well with the Langmuir adsorption model. The carbon foam, obtained from tar pitch derived from RDF and furfural, shows a high adsorption capacity towards nickel ions (203.67 mg/g). The high adsorption capacity could be explained by the properties of the adsorbent—moderately high surface area, micro-mesoporous texture and presence of oxygen-containing surface groups.

**Keywords:** carbon foam; RDF; activation; pore structure; adsorption



**Citation:** Stoycheva, I.; Tsyntsarski, B.; Kosateva, A.; Petrova, B.; Dolashka, P. Assessment of the Possibilities for Removal of Ni (II) from Contaminated Water by Activated Carbon foam Derived from Treatment Products of RDF. *Processes* **2022**, *10*, 570. <https://doi.org/10.3390/pr10030570>

Academic Editors: David W. Mazyck and Federica Raganati

Received: 3 February 2022

Accepted: 8 March 2022

Published: 15 March 2022

**Publisher's Note:** MDPI stays neutral with regard to jurisdictional claims in published maps and institutional affiliations.



**Copyright:** © 2022 by the authors. Licensee MDPI, Basel, Switzerland. This article is an open access article distributed under the terms and conditions of the Creative Commons Attribution (CC BY) license (<https://creativecommons.org/licenses/by/4.0/>).

## 1. Introduction

The presence of heavy metals (Pb, Hg, As, Cd, Ni, Cr, etc.) in industrial waters is a major environmental problem [1]. The presence of nickel in drinking water is due to the leaching of metals in contact with drinking water, such as water pipes and cranks. Nickel can be found also in ground water near nickel ores. Nickel has found extensive applications in steel industry, battery production, metal coatings, electronics, etc. Nickel alloys are thermally stable and resistant towards corrosion. Nickel is a microelement, included in multivitamin tablets.

There are various methods for the purification of water from heavy metal water that are successfully applied: adsorption, extraction, osmosis, ion exchange and precipitation [2,3]. The most effective methods for the removal of pollutants from waters are the adsorption methods using carbon-containing materials [4–7]. Scientists are looking for new and inexpensive adsorbents that can be successfully used for the removal of various contaminants from drinking water.

Carbon foam is a new, cost-effective and promising adsorbent. Its main characteristics that attract the interest of many scientists are the highly developed porous structure (wide range of pores of different size), heat resistance, electro-conductivity and low density.

RDF (Refuse Derived Fuel) is a combination of industrial and household waste that contains flammable materials (as polymers, paper and others.). The essential parameters of RDF are energy content, ash amount and water content. RDF is used as a fuel in the power industry [8,9].

The main focus of this work is to prepare a highly efficient adsorbent carbon foam obtained from a mixture of RDF tar pitch and furfural and to study its potential application in the purification of drinking water from nickel ions.

## 2. Materials and Methods

### 2.1. Preparation of the Adsorbent

A mixture containing tar pitch derived from RDF with a softening temperature of 70 °C, and furfural (in ratio 50:50 wt%), was used as a precursor. Tar pitch derived from RDF was thermally treated at 120 °C, and then furfural was added. A further 68 wt. % HNO<sub>3</sub> by drops was added to the mixture and heated up to 180 °C. The resulting carbonizate was washed with water and then pyrolysed in nitrogen at 600 °C.

The preparation of activated carbon foam was performed by thermo-chemical treatment with water vapor (physical activation with steam or high temperature hydrolysis) at 850 °C of the pyrolyzed samples for 40 min and a rate of temperature rise of 15 °C.

### 2.2. Methods for Characterization

Elemental analysis (C, H, N and S) was carried out with Elementar vario MACRO cube apparatus. The amount of oxygen in the sample was calculated by the difference.

The texture of the obtained carbon material was analyzed using low-temperature N<sub>2</sub> sorption, carried out in an automatic volumetric apparatus Quantachrome Autosorb iQ-C-XR/MP. Prior to nitrogen adsorption, the samples were subjected to outgassing in a vacuum at 300 °C for 8 h.

Thermogravimetry and differential scanning calorimetry were performed on a NET-ZSCH STA449F3 apparatus.

Raman spectra were performed by a Bruker SENTERRA II instrument. Samples were placed onto glass (approximately 10 mg) and analyzed using the vertical objective with magnification of 20x objective in a 180° backscattering arrangement. The Raman spectrometer parameters used to analyze the carbon samples were: 532 nm laser wavelength and an exposure time of 100 s; resolution was 1 cm<sup>-1</sup> for all samples; laser power was 6.5 mW.

FTIR experiments were performed by spectrometer Bruker Vector 22 using pellets with KBr (1:1000), in the wavenumber range 4000–400 cm<sup>-1</sup>, a with resolution of 0.5 cm<sup>-1</sup> and 64 scans.

The morphological study was performed using scanning electron microscope JEOL JSM-6390.

### 2.3. Adsorption

The adsorption activity of carbon foam towards nickel cations was studied as follows: 100 mg carbon was introduced in 0.005 L Ni(NO<sub>3</sub>)<sub>2</sub>.6H<sub>2</sub>O/concentrations 10–40 mg/L/. The initial concentrations of nickel and the equilibrium concentrations were analyzed spectrophotometrically by a Merck Pharo 300 apparatus as dimethylglyoxime complex [10]. pH was adjusted using 0.1 M sodium hydroxide and 0.1 M hydrochloric acid.

## 3. Results

The results for the content of carbon, hydrogen, nitrogen, sulfur and oxygen in carbon foam sample are shown in Table 1.

**Table 1.** Content of elements in activated carbon foam sample.

Sample	C (wt. %)	N (wt. %)	H (wt. %)	S (wt. %)	C/H Ratio (at.)	O (wt. %)
CFoam HNO <sub>3</sub>	85.01	2.81	1.93	0.61	3.67	9.64

Data indicate that a high number of condensation processes, during the synthesis and carbonization of the foam precursor, lead to the formation of condensed aromatic structures, which is related with a high carbon content and low content of hydrogen and oxygen. As a result of these reactions, a larger amount of aromatic compounds was formed, and high molecular structures appeared, leading to increased viscosity of the reaction mixture. The formation of the carbon foam porous structure is influenced by the treatment of the raw material with mineral acids, whereas gas molecules are released. On the other hand, treatment with nitric acid leads to a large number of condensation reactions, and water molecules are evolved from the sample, thus decreasing the amount of H and O. At the same time, the amount of N in the final carbon foam sample increased due to nitric acid treatment.

The  $N_2$  adsorption isotherm and micropore pore size distribution are presented in Figures 1 and 2, respectively. The textural properties are presented in Table 2. It is important to note the short soak time for hydrolysis steam activation (about 40 min). Nevertheless, the resulting activated carbon foam is characterized by a moderate specific surface area of  $474 \text{ m}^2 \text{ g}^{-1}$  and a total pore volume of  $0.297 \text{ cm}^3 \text{ g}^{-1}$ .

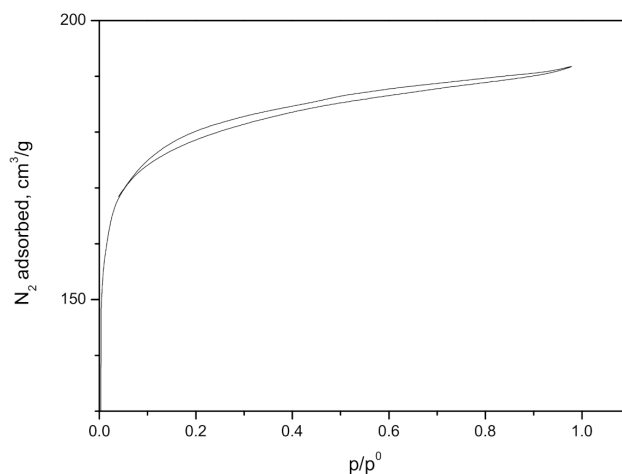


**Figure 1.**  $N_2$  sorption isotherm activated carbon foam sample at  $-196 \text{ }^\circ\text{C}$ .

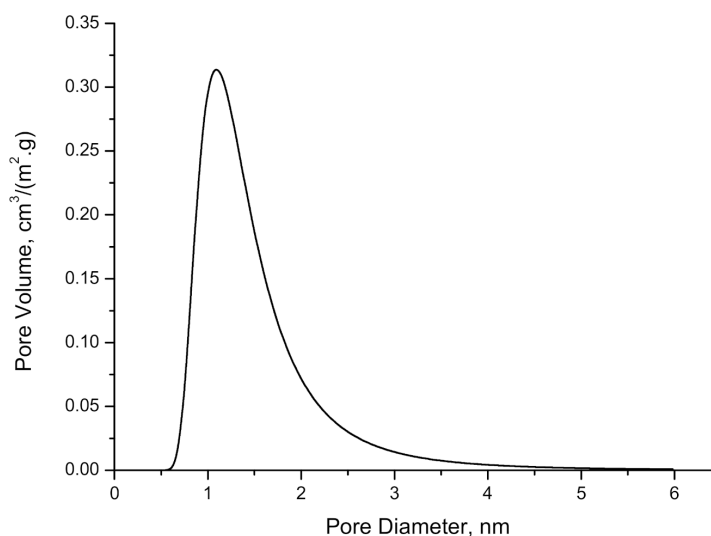


**Figure 2.** Micropore size distribution (Dubinin–Astakhov).

**Table 2.** Textural properties of activated carbon foam.

Sample	$S_{\text{BET}}$ $\text{m}^2/\text{g}$	$V_{\text{total}}$ $\text{cm}^3/\text{g}$	$V_{\text{micro}}$ $\text{cm}^3/\text{g}$	$V_{\text{meso}}$ $\text{cm}^3/\text{g}$
CFoam $\text{HNO}_3$	474	0.297	0.258	0.010

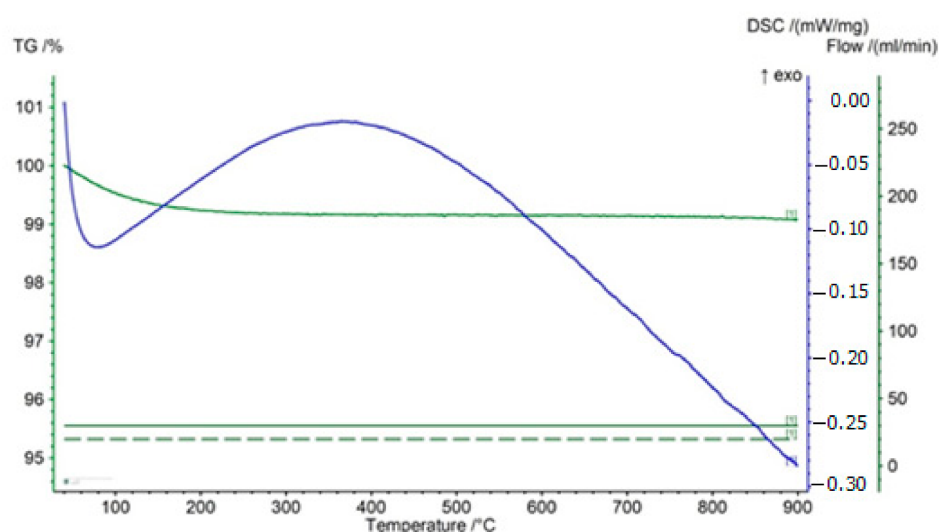
Hydropyrolysis leads to the formation of a carbon foam porous matrix with an open-cell structure and inter-connected micro- /meso-pores.

Porosity has a strong effect on the adsorption properties of activated carbon. The pore structure of the obtained activated carbon was investigated by  $\text{N}_2$  gas sorption. Textural characterization was carried out by measuring the  $\text{N}_2$  sorption isotherms at  $-196\text{ }^\circ\text{C}$ . The nitrogen sorption isotherm of the carbon foam is presented in Figure 1. The analysis of the nitrogen sorption data indicates that carbon foam has a moderately high surface area ( $S_{\text{BET}}$ ) and a well-developed pore structure (Table 2). The part of the isotherms in the range of the relatively lower pressures has a steep increase with a tendency for saturation, which is typical for microporous adsorbents. The  $\text{N}_2$  sorption isotherms obtained correspond to a mixed I-b/IV-a type, according to Brunauer classification, at low pressure. The main textural parameters of the prepared carbon, obtained from the analysis of the nitrogen adsorption isotherms, are compiled in Table 2.

According to IUPAC classification, the isotherm is of mixed I-b/IV-a type, with a hysteresis of H4 type, characteristic for micro-mesoporous material. Type H4 hysteresis is also often associated with narrow slit pores.

Our results show that using the precursor mixture of polyolefin wax and phenol-formaldehyde resin (containing oxygen) leads to activated carbon foam with a high surface area. The pore volume analysis shows that this activated carbon foam has a prevailing content of micropores.

The differential thermogravimetry and differential scanning calorimetry of carbon foam provided valuable data regarding the type of ongoing processes at heat treatment (Figure 3). The DSC and DTG profiles show different processes taking place during the temperature treatment ( $20\text{--}900\text{ }^\circ\text{C}$ ) of the sample. The detected small overall weight loss is most probably due to the presence of aromatic hydrocarbon structures with high thermal stability.

**Figure 3.** TG and DSC analysis of carbon foam sample.

The DSC curve shows a strongly expressed exo-effect in the temperature range of  $150\text{--}600\text{ }^\circ\text{C}$ , which indicates that many exothermic processes run during the temperature treatment of carbon foam.

The analysis of the structure of obtained carbonized carbon foam, including the evaluation of ordering of the crystal structure, is possible due to research using Raman spectroscopy (Figure 4).

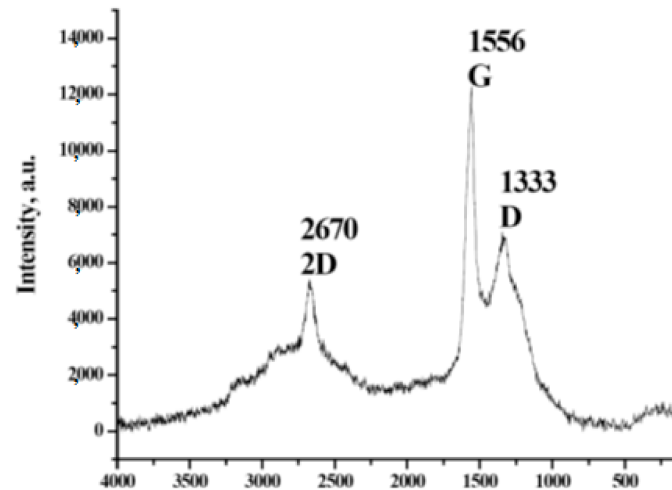


**Figure 4.** Raman spectrum of carbonized carbon foam.

In the Raman spectra obtained for carbon foam, a G bands was observed at  $1556\text{ cm}^{-1}$ . The bands located at the Raman shift at  $1333\text{ cm}^{-1}$  (Figure 4) can be assigned as the so-called D band. As we can see in Figure 4, the G band was much stronger than the D band, which is an indication for the dominant presence of ordered carbon structures. Figures 5 and 6 show Raman spectra of reference and space samples, respectively. Two main Raman bands were detected for both samples—the D band (D for defect, representing the disordered structures) around  $1333\text{ cm}^{-1}$  and the G band located around  $1556\text{ cm}^{-1}$ . The G-band (G for graphite) arises from the stretching of the C–C bond and is common to all  $\text{sp}^2$  carbon systems.

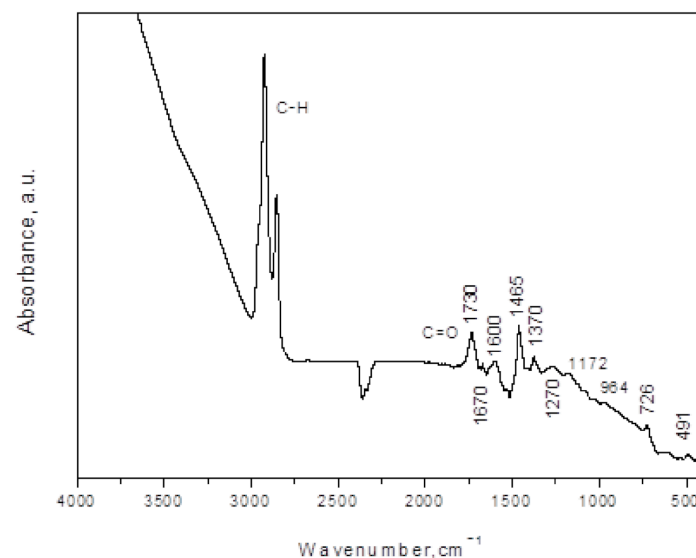


**Figure 5.** FTIR spectra of carbon foam.

IR spectra of the carbon foam sample are presented in Figure 5. The band at  $1709\text{ cm}^{-1}$  could be related to the stretching of C=O in linear aliphatic aldehydes, ketones and carboxyls. The bands around  $1660\text{ cm}^{-1}$  could be due to the aromatic ring stretching of carbonyl groups C=O, C=C bonds or OH groups. The bands in the region of  $1200\text{--}1000\text{ cm}^{-1}$

are due to C–O in ethers structures. The IR spectroscopy results confirm the presence of oxygen-containing groups on the surface, which increase the adsorption properties of activated carbon.

Figure 6 shows the SEM image of carbonized foams. The foam cells are relatively uniform, with a size around 200–300  $\mu\text{m}$ . The foam cells are mainly open, with a size around 300–350  $\mu\text{m}$ . SEM images clearly show that there are cracks in the samples, characteristic for well-developed carbon foam.

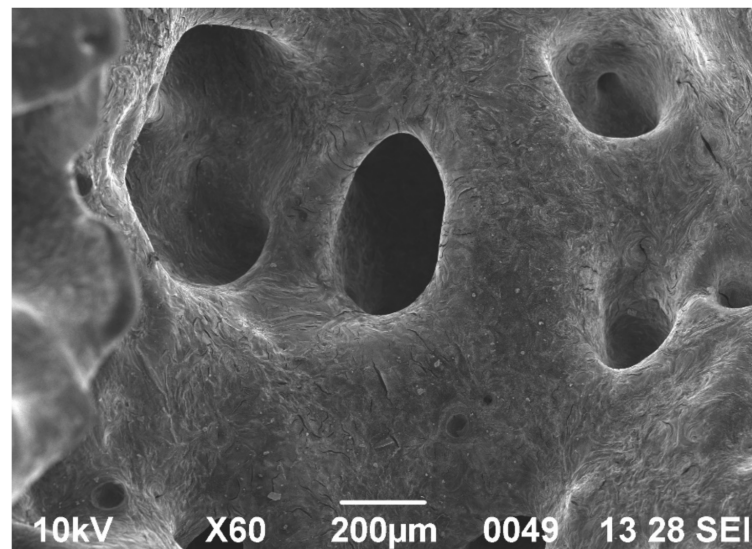


Figure 6. SEM of carbon foam.

#### 4. Adsorption of Nickel Ions in Aqueous Solution

##### 4.1. Langmuir Adsorption Isotherm

The adsorption capacity study is carried out using  $\text{Ni}^{2+}$  concentrations 10–40 mg/L (Figure 7).

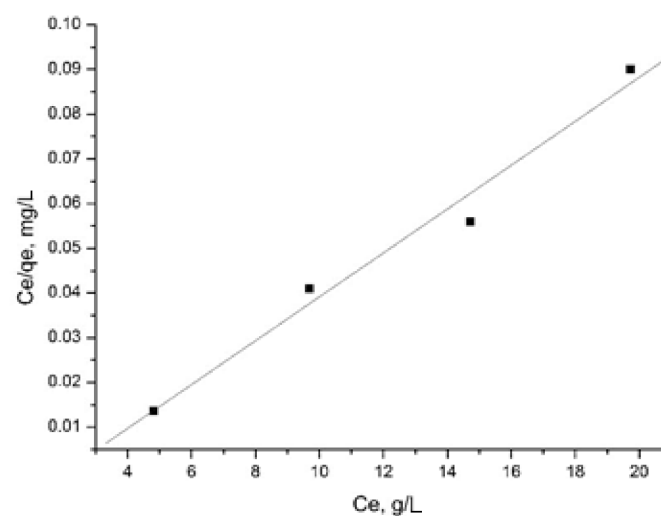


Figure 7. Langmuir adsorption plot of nickel (II) adsorbed by carbon foam. /Ni (II) concentration 10–40 mg/L; time 1 h; adsorbent concentration 0.1 g/50 mL/.

$\text{Ni}^{2+}$  adsorption isotherm is well described by the Langmuir model [11]:

$$C_e/q_e = C_e/q_m + 1/bq_m$$

where  $q_e$ —equilibrium amount of metal ions adsorbed by the adsorbent (mg/g),  $C_e$ —equilibrium metal concentration in the water solution (mg/L);  $q_m$ —maximal adsorption capacity of the adsorbent (mg/g); and  $b$ —constant (L/mg), connected with adsorption affinity.

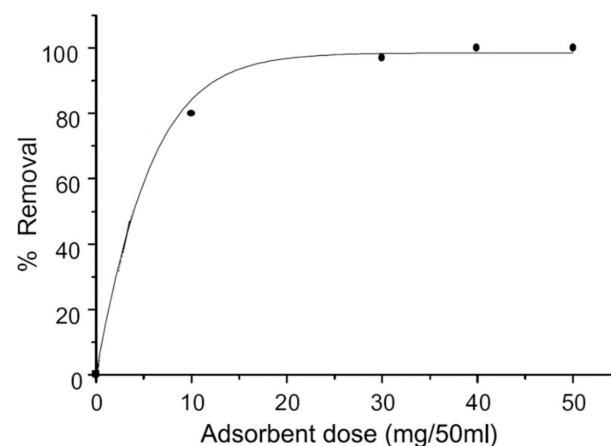
It should be noted that the obtained adsorption capacity of activated carbon from tar pitch derived from RDF and furfural (203.67 mg/g) is much higher than the results from other authors (Table 3).

**Table 3.** Adsorption activity towards Ni (II) of different adsorbents.

Adsorbent Used	$Q_0$ (mg g <sup>-1</sup> )	Literature
Rice hulls	5.60	[12]
Dye treated rice hulls	6.20	[12]
Red-mud	13.69	[13]
Na-ZSM-5-zeolites	1.04	[14]
PNa <sub>2</sub> -ZSM-5-zeolites	1.48	[14]
Almond husk	37.00	[15]
Lignocellulose/Montmorillonite Nanocomposite	94.86	[16]
Polymerized onion skin	7.55	[17]
Peanut hull carbon	53.65	[18]
Granular activated carbon	1.49	[18]
Bituminous coal	6.47	[19]
H <sub>2</sub> O <sub>2</sub> treated coal	8.12	[19]
CF mixture of furfural and industrial tar pitch derived from RDF	203.67	This work

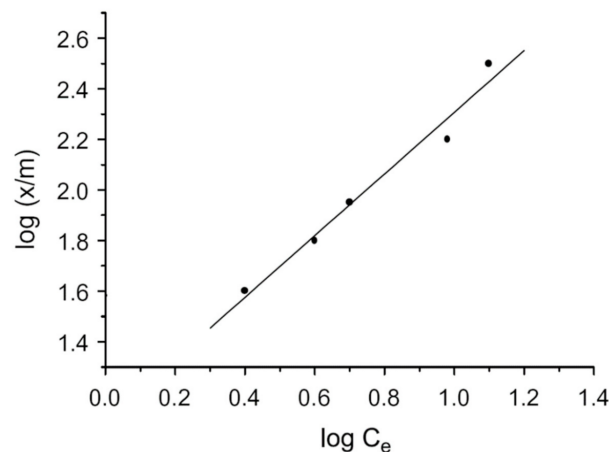
#### 4.2. Freundlich Isotherm

The influence of different doses (5–50 mg per 50 mL solution) on the removal of Ni (II) at fixed initial concentrations of 20 and 40 mg/L Ni<sup>2+</sup> is shown in Figure 8. The increase of carbon dose leads to the enhancement of the percent removal of nickel.



**Figure 8.** Effect of carbon dosage on the removal of Ni (II)/pH 2, time of treatment 1 h/.

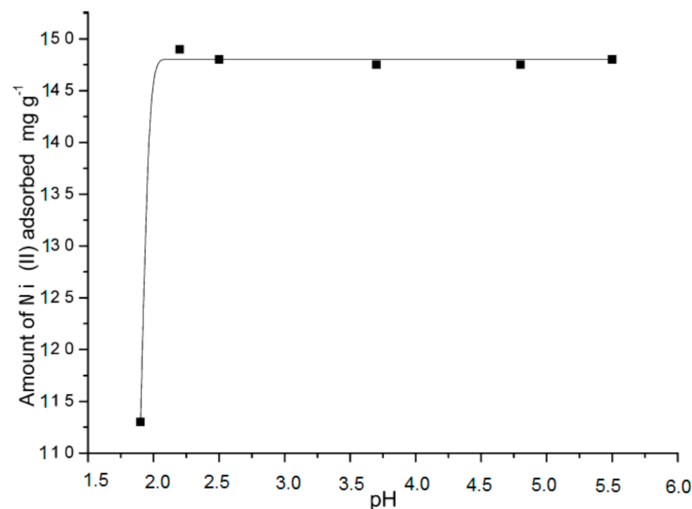
The linear form of Freundlich equation  $\log(x/m) = \lg K_f + \lg C_e/n$  is applied to the results presented at Figure 8 and is shown in Figure 9, whereas  $x$  is the amount of the adsorbed solute (mg),  $m$  is the weight of the adsorbent (g),  $C_e$  is the equilibrium concentration (mg/L),  $n$  is the slope, showing the variation of the adsorption with concentration, and  $K_f$  is the intercept, showing the adsorption capacity of the adsorbent.



**Figure 9.** Freundlich isotherm of Ni (II) adsorption /adsorbent amount 5–50 mg per 50 mL, pH 2, time of treatment 1 h/.

It is well known that the pH of a solution is a critical factor in the adsorption from a solution; not only do carbon surface properties change with variations of the pH, but this parameter can also affect the state of the ionic species in a solution.

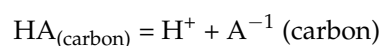
Figure 10 shows the results of the effect of pH on the adsorption of Ni (II) on carbon foam.

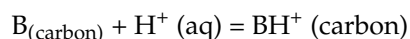


**Figure 10.** Effect of pH on Ni (II) adsorption on the studied carbon/30 min treatment time, 100 mg carbon adsorbent per 100 mL, 5 mg g<sup>-1</sup> Ni (II)/.

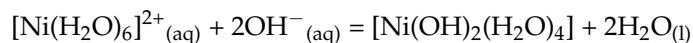
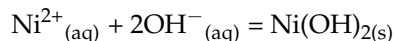
The pH of the solution influences the electrostatic interactions between adsorbent and adsorbate. The desired pH was obtained by adding different amounts of NaOH or HCl solutions. The removal of nickel was found to be maximal at pH > 2. As the pH increases, the surface of the activated carbons is being negatively charged until solution pH > pHPZC, where the number of negative charges becomes predominant in the carbon surface. At this point, the fall in the uptake is due to the repulsive interactions that appear between the anionic form of the adsorbates and the charges on the carbon surfaces.

There are several plausible mechanisms for metal adsorption: ion-exchange, complexation (both specific adsorption pathways) or a combination of both. For the ion-exchange process, taking into account that the surface of carbon foam is covered with weak acidic (HA) and basic (B) sites, we can assume that the ionization of these sites follows the reaction schemes shown below:





In aqueous solution, nickel forms the green stable hexaaqua nickel(II) ion,  $[\text{Ni}(\text{H}_2\text{O})_6]^{2+}(\text{aq})$ . Ni (II) cation adsorption on the carbon surface may be described by the following reactions:



At higher concentrations, a complexation with oxygen containing functional groups can be observed. The presence of basic oxygen functionalities on the carbon surface seems to be needed to enhance the amount adsorbed via ion-exchange and complexation with the nickel ionic species.

The high adsorption capacity could be explained by the properties of the adsorbent—moderately high surface area, micro-mesoporous texture and presence of oxygen-containing surface groups.

## 5. Conclusions

The thermo-oxidative modification with  $\text{HNO}_3$  of a mixture containing RDF tar pitch and furfural leads to polycondensation and polymerization processes, which cause appropriate changes in the composition and viscosity of the reaction mixture. As a result, carbon foam, which possess a well-developed pore structure with prevailing macropores, is synthesized.

The physicochemical composition of the precursor mixture affects the characteristics of the carbon foam synthesis product. Increased furfural amount in the reaction mixture leads to the formation of a homogenous carbon foam porous structure.

The formation of a big number of oxygen-rich species during thermal oxidation treatment with  $\text{HNO}_3$  causes polycondensation reactions and the formation of a larger amount of aromatic compounds and high molecular structures. The carbon foam treated with  $\text{HNO}_3$  using nitric acid is distinguished by an ordered structure. Further hydrolysis leads to the formation of a carbon foam porous matrix with an open-cell structure and inter-connected micro- /meso- pores.

The adsorbent has very good surface properties and the ability to remove Ni (II) from aqueous solution. The surface characteristics strongly depend on the preparation conditions. Carbon foam exhibits a high capacity to adsorb nickel ions from aqueous solution—203.67 mg/g. The adsorption of Ni (II) follows Langmuir isotherm and Freundlich isotherms.

The high adsorption capacity could be explained by the properties of the adsorbent—moderately high surface area, micro-mesoporous texture and the presence of oxygen-containing surface groups.

**Author Contributions:** Investigation, I.S., B.T., A.K., B.P. and P.D.; writing—original draft preparation, I.S., B.T. and P.D.; writing—review and editing, I.S., B.T., B.P. and P.D.; supervision, I.S. and P.D. All authors have read and agreed to the published version of the manuscript.

**Funding:** Project BG05M2OP001-1.002-0019: “Clean technologies for sustainable environment—water, waste, energy for circular economy”, financed by the Operational programme “Science and Education for Smart Growth” 2014–2020, co-financed by the European union through the European structural and investment funds. The authors acknowledge financial support for this work by the Bulgarian National Science Fund, grant number KP-06-M37/3 from 6 December 2019.

**Institutional Review Board Statement:** The study was conducted in accordance with the The European Code of Conduct for Research Integrity and the Declaration of Helsinki, and approved by the Ethics Committee of INSTITUTE OF ORGANIC CHEMISTRY WITH CENTRE OF PHYTOCHEMISTRY (protocol code IOCCP-005 and date of approval 23.04.2019).

**Informed Consent Statement:** Informed consent was obtained from all subjects involved in the study.

**Data Availability Statement:** The data presented in this study are available on request from the corresponding author.

**Conflicts of Interest:** The authors declare no conflict of interest.

## References

1. Masindi, V.; Muedi, K. Environmental Contamination by Heavy Metals. In *Heavy Metals*; Chapter 7; IntechOpen: London, UK, 2018; pp. 115–134.
2. Nasiruddin, M.; Bhutto, S.; Wasim, A.A.; Khurshid, S. Removal studies of lead onto activated carbon derived from lignocellulosic *Mangifera indica* seed shell. *Desalination Water Treat.* **2016**, *57*, 11211–11220. [[CrossRef](#)]
3. Gupta, V.K.; Jain, C.K.; Ali, I.; Sharma, M.; Saini, V.K. Removal of cadmium and nickel from wastewater using bagasse fly ash—A sugar industry waste. *Water Res.* **2003**, *37*, 4038–4044. [[CrossRef](#)]
4. Di Natale, F.; Lancia, A.; Molino, A.; Dinatale, M.; Karatza, D.; Musmarra, D. Capture of mercury ions by natural and industrial materials. *J. Hazard. Mater.* **2006**, *132*, 220–225. [[CrossRef](#)] [[PubMed](#)]
5. Yin, C.Y.; Aroua, M.K.; Daud, W.M.A.W. Polyethyleneimine impregnation on activated carbon: Effects of impregnation amount and molecular number on textural characteristics and metal adsorption capacities. *Mater. Chem. Phys.* **2008**, *112*, 417–422. [[CrossRef](#)]
6. Nabais, J.V.; Carrott, P.J.M.; Ribiero Carrott, M.M.L.; Belchior, M.; Boavida, D.; Dially, T.; Gulyurtlu, I. Mercury removal from aqueous solution and flue gas by adsorption on activated carbon fibres. *Appl. Surf. Sci.* **2006**, *252*, 6046–6052. [[CrossRef](#)]
7. Zhang, S.; Wang, J.; Zhang, Y.; Ma, J.; Huang, L.; Yu, S.; Chen, L.; Song, G.; Qiu, M.; Wang, X. Applications of water-stable metal-organic frameworks in the removal of water pollutants: A review. *Environ. Pollut.* **2021**, *291*, 118076. [[CrossRef](#)] [[PubMed](#)]
8. Akdag, A.; Atımtay, A.; Sanina, F. Comparison of fuel value and combustion characteristics of two different RDF sample. *Waste Manag.* **2016**, *47*, 217–224. [[CrossRef](#)] [[PubMed](#)]
9. Srisaeng, N.; Tippayawong, N.; Tippayawongm, K. Energetic and Economic Feasibility of RDF to Energy Plant for a Local Thai Municipality. *Energy Procedia* **2017**, *110*, 115–120. [[CrossRef](#)]
10. Kadirvelu, K.; Thamaraiselvi, K.; Namasivayam, C. Adsorption of nickel(II) from aqueous solution onto activated carbon prepared from coirpith. *Sep. Purif. Technol.* **2001**, *24*, 497–505. [[CrossRef](#)]
11. Condon, J. Surface Area and Porosity Determinations by Physisorption. In *Measurement, Classical Theories and Quantum Theory*; Elsevier: Amsterdam, The Netherlands, 2020.
12. Suemitsu, R.; Venishi, R.; Akashi, I.; Nakana, M. The use of dyestuff-treated rice hulls for removal of heavy metals from waste water. *J. Appl. Polym. Sci.* **1986**, *31*, 75–83. [[CrossRef](#)]
13. Hannachi, Y.; Shapovalov, N.A.; Hannachi, A. Adsorption of Nickel from aqueous solution by the use of low-cost adsorbents. *Korean J. Chem. Eng.* **2010**, *27*, 152–158. [[CrossRef](#)]
14. Panneerselvam, P.; Sathya Selva Bala, V.; Thinakaran, N.; Baskaralingam, P.; Palanichamy, M.; Sivanesan, S. Removal of Nickel(II) from Aqueous Solutions by Adsorption with Modified ZSM- 5 Zeolites. *J. Chem.* **2009**, *6*, 729–736. [[CrossRef](#)]
15. Hasar, H. Adsorption of nickel(II) from aqueous solution onto activated carbon prepared from almond husk. *J. Hazard. Mater.* **2003**, *97*, 49–57. [[CrossRef](#)]
16. Zhang, X.; Wang, W. Adsorption and Desorption of Nickel(II) Ions from Aqueous Solution by a Lignocellulose/Montmorillonite Nanocomposite. *PLoS ONE* **2015**, *10*, e0117077. [[CrossRef](#)] [[PubMed](#)]
17. Kumar, P.; Dara, S.S. Binding Heavy Metal Ions with Polymerized Onion Skin. *J. Polym. Sci.* **1981**, *19*, 397–402. [[CrossRef](#)]
18. Periasamy, K.; Namasivayam, C. Removal of nickel(II) from aqueous solution and nickel plating industry wastewater using an agricultural waste: Peanut hulls. *Waste Manag.* **1995**, *15*, 63–68. [[CrossRef](#)]
19. Singh, D.; Rawat, N.S. Adsorption of heavy metals on treated and untreated low grade bituminous coal. *J. Chem. Technol. Biotechnol.* **1997**, *4*, 39–41.